γ-Tubulin interacts with E2FA, E2FB and E2FC transcription factors, regulates proliferation and endocycle in Arabidopsis

Kállai B.M.[3#], Kourová H.[1#], Chumová J.[1], Papdi C.[2], Trögelová L.[1], Kofroňová O.[1], Hozák P.[5], Filimonenko V.[5], Mészáros T.[3], Magyar Z.[4], Bögre L.[2], Binarová P.[1]

[1]Institute of Microbiology of the Czech Academy of Sciences, Vídeňská 1083, Prague 4, 142 20, Czech Republic

[2]Department of Biological Sciences, Centre for Systems and Synthetic Biology, Royal Holloway University of London, Egham Hill, Egham, TW20 0EX, UK

[3]Department of Medical Chemistry, Molecular Biology and Pathobiochemistry, Semmelweis University, Tűzoltó u. 37-47, H-1094 Budapest, Hungary

[4]Institute of Plant Biology, Biological Research Centre, Temesvári krt. 62, POB 521, H-6701 Szeged, Hungary

[5]Institute of Molecular Genetics of the Czech Academy of Sciences, Vídeňská 1083, Prague 4, 142 20, Czech Republic

# both authors contributed equally

Author for correspondence:
Pavla Binarová
Tel: +420296442130
Email: binarova@biomed.cas.cz

Highlight

γ-Tubulin interacts with E2F transcription factors and acts as a repressor of E2F target genes regulating G1/S, G2/M and the switch to endocycle in plants.

Abstract

γ-Tubulin is associated with microtubule nucleation, but evidence is accumulating in eukaryotes that it functions also in nuclear processes and in cell division control that are independent of its canonical role. We found that in *Arabidopsis thaliana* γ-tubulin interacts specifically with E2FA, E2FB, and E2FC transcription factors both *in vitro* and *in vivo*. The interaction of γ-tubulin with the E2Fs is not reduced in the presence of the dimerization partners (DPs) and, in agreement, we found that γ-tubulin interaction with E2Fs does not require the dimerization domain. γ-Tubulin associates with the promoters of E2F-regulated cell cycle genes in an E2F dependent manner, likely in complex with the E2F/DP heterodimer. The upregulation of E2F targets; *PCNA, ORC2, CDKB1;1* and *CCS52A* under γ-tubulin silencing suggests a repressive function for γ-tubulin at G1/S, G2/M and endocycle, which is consistent with an excess of cell division in some cells and enhanced endoreduplication in others in the shoot and young leaves of γ-tubulin RNAi plants. Altogether, our data show ternary interaction of γ-tubulin with E2F/DP heterodimer and suggest a repressive role for γ-tubulin with E2Fs in controlling mitotic activity and endoreduplication during plant development.

Keywords: Arabidopsis, E2F transcription factors, endoreduplication, gene expression, proliferation, γ-tubulin

Introduction

γ-Tubulin is a highly conserved microtubule nucleator in eukaryotic cells. Microtubule independent role of γ-tubulin in cell cycle regulation and in nuclear processes shows γ-tubulin as a multifunctional protein (Oakley *et al.*, 2015). Presence of γ-tubulin in nuclei of plant (Binarova *et al.*, 2000) and animal cells (Horejsi *et al.*, 2012) suggested its nuclear functions. γ-Tubulin interacts with DNA repair protein Rad51 (Lesca *et al.*, 2005), with the tumour suppressor protein C53 (Horejsi *et al.*, 2012) and forms well-characterized complex with BRCA1 (Gomez and Hergovich, 2014). Evidence was provided for the role of γ-tubulin in chromatin remodelling (Vazquez *et al.*, 2008) and in transcription (Hoog *et al.*, 2011). Functions of γ-tubulin in nuclei organization through interaction with lamins (Rossello *et al.*, 2016) and SUN proteins (Chumova *et al.*, 2019) are suggested. Defective cell cycle progression and coordination of mitotic events were observed in γ-tubulin mutants of *S. pombe* (Hendrickson *et al.*, 2001) and in *Aspergillus* (Prigozhina *et al.*, 2004). *Aspergillus* γ-tubulin mutants showed impaired inactivation of anaphase promoting complex (APC) and coordination of mitosis with spindle assembly checkpoint (Edgerton-Morgan and Oakley, 2012; Edgerton *et al.*, 2015). In acentrosomal plant cells, γ-tubulin is broadly distributed in the cytoplasm with microtubules and membranes and has a role in microtubule nucleation from dispersed sites (Binarova *et al.*, 2006; Pastuglia *et al.*, 2006). Besides its microtubule nucleation function, microtubule independent roles of γ-tubulin in plant cell division also have been suggested (Binarova *et al.*, 2006; Pastuglia *et al.*, 2006), but molecular mechanisms behind remain to be uncovered.

γ-Tubulin interacts with the transcription factor E2F1 and modulates the progression through G1/S phase of the cell cycle in mammalian cells (Hoog *et al.*, 2011). In *Arabidopsis thaliana* there are three E2Fs; E2FB and E2FA are positive regulators for cell proliferation and endoreduplication, respectively, while E2FC suppresses cell division (Magyar *et al.*, 2016). E2Fs make heterodimers with either dimerization partner A or B (DPA and DPB) proteins in order to bind to target promoters (Magyar *et al.*, 2000). Arabidopsis E2Fs are controlled by the RETINOBLASTOMA-RELATED (RBR) protein and the E2F-binding activity of RBR is regulated through phosphorylation by the CYCLIN-DEPENDENT-KINASE A;1 (CDKA;1) /CYCLIN-Ds (CYCDs) /KIP-RELATED PROTEINs (KRPs). This E2F-RBR system controls the expression of genes involved in cell-cycle progression, DNA replication, and chromatin dynamics. The E2F-RBR pathway was primarily linked with the regulation of cell cycle entry during the G1/S progression, but its function was also associated with G2/M regulation, as part of the evolutionary conserved multiprotein DP, RB-like, E2F, and MuvB (DREAM)

complex (Magyar *et al.*, 2016). In addition, E2FA, when released from RBR repression, is important for the switch from cell division to endoreduplication (De Veylder *et al.*, 2002; Magyar *et al.*, 2012).

In this work, we decided to characterize whether microtubule independent role of plant γ-tubulin in cell division (Binarova *et al.*, 2006) is performed through γ-tubulin interaction with plant E2F transcription factors. Our data suggest that γ-tubulin has a regulatory role together with E2FA, E2FB or E2FC to coordinate cell division with endocycle during plant growth and development.

Material and Methods

Vector construction and plant transformation

As described in details in (Binarova *et al.*, 2006) the γ-tubulin RNAi vector was constructed by generating an inverted hairpin loop of a 722-bp fragment corresponding to nucleotides 700 to 1425 of the *Arabidopsis thaliana* TubG1. Shortly the PCR fragment was cloned directly into pGEM-T vector (Promega) and cloned into pART69 to generate the RNAi intermediate construct and transferred into ethanol inducible vector to generate the pGreenAlcA:TubG1-RNAi. Alternatively, a hairpin from 552-bp fragment corresponding to nucleotides 292 to 844 of the AtTubG1 sequence was used. The PCR fragments were cloned into pHANNIBAL (Wesley *et al.*, 2001) and the resulting cassette consisting of CaMV35S promoter, two hairpin arms separated with an intron and OCS terminator was transferred to the binary vector pART27 using a NotI cleavage. Gene specific primers used for pArt27:TubG1-RNAi construction are listed in Table S1. *Arabidopsis thaliana* (Col-0) was transformed by the floral dip in suspension of *Agrobacterium tumefaciens* GV3101.

To construct the pgE2FB- and pgE2FC-GFP translational fusions, the promoter regions and the genomic clones including exons and introns were amplified from Col-0 genomic DNA using the primer combinations described in Table S1. In both cases, the genomic sequences were fused at the 3' prime end with the coding sequence of GFP in a pGreenII-based pGII0125 destination vector (Galinha *et al.*, 2007) by using the Invitrogen 3 way gateway system (Invitrogen, USA). Transgenic plants were generated as described before (Henriques *et al.*, 2010).

Plant material and growth condition

Arabidopsis thaliana ecotype Columbia (Col-0) wild type (WT), pArt27:TubG1-RNAi, pGreenAlcA:TubG1-RNAi (SEM analyses), *e2fa-2;e2fb-1* double mutant (Heyman *et al.*,

2011), and lines expressing GFP-tagged E2Fs under the control of their own promoters pgE2FA-GFP (Henriques *et al.*, 2010), pgE2FB-GFP and pgE2FC-GFP were used. Seeds were sterilised and grown vertically on MS agar plates with appropriate selection (Kohoutova *et al.*, 2015) under 16 h : 8 h, light : dark regime. For anti-microtubule drug treatment, MS agar medium was supplied with 1 µM amiprophosmethyl (APM, Duchefa Biochemie A0185) from stock solution in DMSO. Plants were observed at the developmental stage of 11 das (days after sowing).

Interaction studies with *in vitro* translated proteins

The coding regions of γ-tubulin, DPA, DPB, E2FA, E2FB, E2FC, and MYB66 were inserted into pEU3-NII-HLICNot and pEU3-NII-GLICNot vectors by ligation-independent cloning. The coding region of γ-tubulin was inserted into a pEU3-NII-HxHLICNot vector (data not published) encoding a double-hexahistidine (His_{12}) tag to increase the sensitivity of detection (Khan *et al.*, 2006). The truncated E2F mutants were amplified from the wild type E2F containing vectors by using primers listed in Table S2. The vector constructs were used for *in vitro* translation as described previously (Nagy and Meszaros, 2014).

E2F/γ-tubulin interactions were investigated with pull-down assay by using 1.875 µl of Pierce Glutathione Magnetic Beads (Thermo Scientific) and 30 µl of His_6-γ-tubulin and GST-E2FA/B/C containing *in vitro* co-translation mixtures. Prior to the 1 h incubation with the beads, the translation mixtures were diluted six times with Wash Buffer (125 mM Tris, 150 mM NaCl, 0.5% Triton-X, pH 8). The specificity of E2F/γ-tubulin interaction was demonstrated by mixing and incubating 20 µl of GST-MYB66/E2FA and 40 µl of His_{12}-γ-tubulin containing *in vitro* translation mixtures for 1 h at room temperature and pulling down the complexes with 2.5 µl of Pierce Glutathione Magnetic Beads. Following the pull-down, the beads were split and washed with either 150 mM or 500 mM NaCl containing Wash Buffer. The DP/γ-tubulin competition experiments were implemented by mixing and incubating 30 µl His_6-DPA/B containing translation mixture and 1.875 µl of Pierce Glutathione Magnetic Beads pre-coated with E2F/γ-tubulin complexes for 1 h at room temperature. Interaction between the truncated E2FA/B/C proteins and DPB/γ-tubulin was demonstrated by mixing and incubating 15 µl of truncated GST-E2FA/B/C and 15 µl of His_6-DPB/γ-tubulin containing *in vitro* translation mixtures for 1 h at room temperature and pulling down the complexes with 1.875 µl of Pierce Glutathione Magnetic Beads. The beads were washed with 250 mM NaCl containing Wash Buffer.

The samples were subjected to SDS-PAGE and the proteins were transferred to PVDF membrane by semi-dry blotting. The membranes were blocked with 5% non-fat milk powder in PBS containing 0.05% Tween-20. The labelled proteins were detected either directly by anti-polyHis-POD (Sigma) diluted 1:2,000 or by rabbit anti-GST (Upstate) diluted 1:2,000 and secondary antibody goat anti-rabbit-HRP (Cell Signaling) diluted 1:5,000.

dsDNA binding site studies with ALPHA and Electrophoretic Mobility Shift Assay

Complementary oligonucleotides with Cy5 or biotin labelling on the upper strand and 3' inverse dT modification on the lower strand were synthesized to generate the consensus E2F-binding site and its mutant version (IBA Life Sciences). Sequences of wild type E2F and mutated binding sites: upper strand 5'-TTTCCCGCCAAtagc -3'; lower strand 5'-gctaTTGGCGGGAAA-3' and 5'-TTTCCaaCCAAtagc-3'; 5'-gctaTTGGttGGAAA-3', respectively. Lower case letters represent overhanging and mutated nucleotides (modified from Magyar *et al*., 2012). The oligonucleotides were hybridized in annealing buffer (100 mM Tris, 500 mM NaCl, pH 8) to create 50 µM dsDNA stock solutions.

ALPHA (Amplified Luminescence Proximity Homogeneous Assay) sample mixtures were assembled in 384-well plate at 20 µl final volume (AlphaPlate 384 SW, Perkin Elmer). The measurements were implemented in PBS diluted wheat-germ translation mixtures completed with BSA and salmon sperm DNA to reach 1 mg/ml and 0.1 µg/ml final concentrations, respectively. AlphaScreen Streptavidin Donor and Nickel chelate Acceptor beads (Perkin Elmer) were used at 20 µg/ml final concentration. Diverse variations of *in vitro* translated His_6-E2FB, His_6-DPB, and GST-γ-tubulin (approximately 50 ng of them) were mixed and incubated at room temperature for 2 h. Following the addition of biotin labelled dsDNA coated donor beads, the mixtures were incubated for 30 minutes. Next, the acceptor beads were added, and the samples were incubated for a further hour. The luminescent signal (counts per second, cps) was measured by using the default ALPHA settings of Enspire (Perkin Elmer) plate reader.

Electrophoretic Mobility Shift Assay (EMSA) was carried out by using 5% native polyacrylamide gel (29:1 acrylamide:bisacrylamide) polymerized in 50 mM Tris, 0.38 M glycine and 2 mM EDTA, pH 7.5 containing buffer. The His_6-E2FB, His_6-DPB and GST-γ-tubulin were produced by wheat-germ *in vitro* translation. The respective Cy5 labelled dsDNAs were incubated with 1-1 µl of total translation mixtures at 5 µM final DNA

concentration for 1 h at room temperature in EMSA buffer (250 ng of poly(dI-dC), 10 mM Tris, 50 mM KCl, 1 mM DTT and 1% Tween-20, pH 7.5). The samples were loaded into native polyacrylamide gel after mixing them with loading buffer without dyes and separated at 70V in TBE buffer. The gels were imaged by using a Typhoon scanner.

Super-shift assays were performed as described by Hsieh *et al.* (2016) with slight modifications. The GST-E2FA, untagged DPB, and His_6-γ-tubulin were produced by wheat-germ *in vitro* translation. GST-E2FA and His_6-γ-tubulin were co-translated, GST-E2FA and untagged DPB were pre-incubated for 90 minutes, then 1.6 µl of the respective translation mixtures were incubated for further 90 minutes prior to addition of DNA. The super-shift assay mixtures contained 1 µl anti-polyHis antibody (Sigma, H1029), 1 µg/ml poly(dI-dC) and 0.1 µM Cy5 labelled WT DNA. Of note, the available GST antibodies did not work in the super-shift assay; thus, His_6-γ-tubulin was used to demonstrate DNA binding of heterotrimer complex. All the *in vitro* interaction studies were performed in at least five independent experiments.

Protein purification, Immunoblotting, and Immunoprecipitation

Proliferating or non-proliferating conditions were induced by transfer of Arabidopsis seedlings expressing GFP-tagged E2Fs to MS liquid medium containing 2% or 0% sucrose, respectively, for 6 h. Total protein was extracted from Arabidopsis seedlings as described (Magyar *et al.*, 1997) but protease inhibitor cocktail (Sigma-Aldrich) was used instead of unique protease inhibitors. Immunoprecipitations (IPs) by using GFP-Trap coupled magnetic beads (ChromoTek) were carried out according to (Magyar *et al.*, 2012). Bound proteins were separated on SDS-PAGE and immunoblotting assays have been carried out as described (Henriques *et al.*, 2010). Antibodies used in immunoblotting experiments: anti-γ-tubulin plant specific antibody AthTU (Drykova *et al.*, 2003), anti-DPA (Magyar *et al.*, 2005), anti-DPB (Umbrasaite *et al.*, 2010), anti-GFP monoclonal mouse (Roche). Five independent IP experiments were performed and representative images are shown.

Chromatin immunoprecipitation (ChIP)

For ChIP in seedlings, wild type (Col-0) and *e2fa-2;e2fb-1* double mutant plants were grown on sucrose-free media in 12 h light : 12 h dark conditions. In the morning of the 12th day, half of the plants of both genotypes was kept in dark for 4 more hours (extended dark). 3 g of the 'extended dark' and 'light' plants were crosslinked with 1% formaldehyde. For ChIP in cell culture, 1 g of exponentially grown Col-0 cells (3 days after subculturing) were crosslinked

with 1% formaldehyde. Crosslinking and chromatin isolation were performed based on (Saleh *et al.*, 2008). For sonication of the chromatin, BioRupter (Diagonade) was used with 30 s on/off cycles for ten times at high mode. Chromatin fragments were precipitated using 15 µl anti-γ-tubulin antibody and collected with Protein A agarose/salmon sperm DNA (Millipore). The purified DNA was used in qPCR reactions to amplify promoter regions with specific primers listed in Table S1. Relative enrichment was calculated by dividing the antibody immunoprecipitation signals with the no-antibody signals. Three independent experiments were performed.

RNA extraction and Q-RT-PCR

Total RNA was extracted from whole plant tissues using RNeasy Mini Kit (Qiagen), cDNA synthesis was carried out on 1 µg RNA with Maxima First Strand cDNA synthesis kit with dsDNase (Thermo Scientific). For the qPCR reactions, Sybr Green JumpStart Taq ReadyMix (Sigma) was used and the reactions were performed using Rotor-Gene Q (Qiagen). We used actin as a reference gene in all Q-RT-PCR experiments as described in (Horvath *et al.*, 2017). Raw data were analysed with the delta-delta CT method. Gene specific primers used for Q-RT-PCR analysis are listed in Table S1. Three independent experiments were performed.

Phenotype analyses of γ-tubulin RNAi plants

Immunofluorescence labelling and fluorescence microscopy: Slide preparation of squashed Arabidopsis seedlings and immunolabelling was performed as described in (Horvath *et al.*, 2017) using anti-α-tubulin (Abcam, 1:1,000) and anti-mouse Alexa Fluor 488 (1:600) antibodies. Chromatin was counterstained with DAPI. Images were obtained by confocal imaging system Olympus IX-81 FV-1000 as decribed in (Kohoutova *et al.*, 2015). Images were analyses and prepared using FV10 ASW2.0 (Olympus) and Adobe Photoshop/Illustrator CS4 (Adobe System), respectively. Cell counting was performed on immunolabelled mesophyll cells of WT and γ-tubulin RNAi leaves. Cells were counted manually in randomly selected areas defined by 1,000 µm x 1,000 µm square using ImageJ software.

EdU labelling: EdU (5-Ethynyl-2´-deoxyuridine) labelling of whole mount seedlings was performed using Click-iT EdU Alexa Fluor 488 HCS Assay (Molecular Probes) according to (Horvath *et al.*, 2017). Seedlings were incubated in liquid medium with EdU pulse with the dilution of 1:1,000 for 1 h.

Flow cytometry: Nuclei were isolated from WT control (Col-0) and γ-tubulin RNAi seedlings as described in (Doskocilova *et al.*, 2013) using Partec CyStain UV precise P kit (Partec) and flow cytometry was measured on a BD LSRII (BD Biosciences) with a solid state laser (excitation 405 nm) and 450/50 band pass filter. Data evaluation was performed in FlowJo from at least six independent experiments. Endoreduplication index (EI) was determined from percentage values of each C-level with formula: EI = [(0 x % 2C) + (1 x % 4C) + (2 x % 8C) + (3 x % 16C) + (4 x % 32C)] / 100 (Radziejwoski *et al.*, 2011). Chromocentra were labelled and counted as described previously by Doskocilova *et al.* (2013). Phenotype analyses were performed from at least six independent experiments and representative images are shown.

Transmission electron microscopy (TEM)

Root tips of 6 days old *Arabidopsis thaliana* expressing GFP-tagged E2FA under its own promoter were high-pressure frozen in Leica EM PACT2 using 200 mM sucrose in 10 mM Tris buffer, pH 6.6, as a cryoprotectant. Frozen samples were transferred under liquid nitrogen to an automatic freeze-substitution machine (Leica EM AFS2 equipped with Leica EM FSP) and freeze-substitution was done using: dehydrated acetone containing 0.2% uranyl acetate, 0.2% glutaraldehyde and 5% water for 24 h with gradual temperature increase to -80°C, 24 h at -80°C, and increased to -50°C during following 30 h. The mixture was replaced with pure dehydrated acetone and kept for 6 h at -50°C followed by -45°C during 4 h. Samples were then infiltrated with Lowicryl HM20 (Polysciences, Inc.) resin at -45°C: 33% mixture with acetone for 12 h, 66% resin in acetone for 12 h, and three replacements of pure resin for 12, 12 and 11 h. The resin was polymerized using UV light, starting at -45°C with gradual temperature increase to -35°C during 24 h, increased to 20°C during 1 h, and the polymerization continued for next 72 h.

Sections (70–90 nm) were cut using Ultramicrotome Leica EM UC6 with a diamond knife (Diatome AG, Biel, Switzerland) and mounted on gilded copper slots with a Formvar film. To block unspecific immunogold labelling slots were pre-incubated with 10% normal goat serum (Invitrogen), 0.2% cold water fish skin gelatin and 1% BSA in PBS with 0.1% Tween 20, pH 7.4 (PBTB) for 20 minutes. The sections were incubated with chicken anti-GFP antibody diluted 1:100 and rabbit anti-γ-tubulin (plant specific antibody, Drykova et al., 2003, or DQ-19, Sigma-Aldrich) in PBTB containing 0.2% cold water fish skin gelatin for 1 h, washed in 0.005% Tween 20 in PBS, pH 7.4 (PBT), and incubated for 1 h with 6-nm gold-conjugated donkey anti-chicken IgG and 12-nm gold-conjugated goat anti-rabbit IgG (Jackson ImmunoResearch Laboratories Inc., West Grove, PA, USA), diluted each 1:30 in PBTB,

0.2% cold water fish skin gelatin. Control incubations were performed without primary antibody. The slots were observed in FEI Morgagni 268 transmission electron microscope at 80 kV equipped with Mega View III CCD camera (Olympus) or in FEI Tecnai 20 G2 electron microscope equipped with Gatan 863 Tridiem Imaging Filterand Model 894 UltraScan 1000 camera.

Scanning Electron Microscope (SEM)

Arabidopsis leaves were fixed with 3% (w/v) glutaraldehyde in cacodylate buffer, pH 7.2, washed in the same buffer. Then the samples were dehydrated in an alcohol series (25%, 50%, 75%, 90%, 96%, and 100%) followed by absolute acetone and dried in a critical-point device (Balzers 010, Balzers Union Ltd., Lichtenstein). The dried samples were mounted onto aluminum stubs, sputter-coated with gold (Polaron SC 510, Watford, U.K.) and examined on an Aquasem (Tescan, Brno, Czech Republic) scanning electron microscope at 15 kV in high vacuum mode.

Accession numbers: TubG1, At3g61650; E2FA, At2g36010.3; E2FB, At5g2220.2; E2FC, At1g47870.1; DPA, At5g02470.1; DPB, At5g03415.1; MYB66, At5g14750.1; CDKB1;1, At3g54180; CYCD3;1, At4g34160; CCS52A2, At4g11920; PCNA1, At1g07370; RBR, At3g12280; ORC2, At2g37560.

Results

γ-Tubulin binds to E2FA, E2FB and E2FC proteins *in vitro*

Our previous finding on the nuclear localization of γ-tubulin and the meristem organisation phenotypes of γ-tubulin silenced plants (Binarova *et al.*, 2000; Binarova *et al.*, 2006) implied a cell cycle-related function for γ-tubulin. This is consistent with reports on animal cells, where γ-tubulin associates with E2F1 to regulate cell proliferation (Hoog *et al.*, 2011). To test whether γ-tubulin specifically interacts with E2Fs also in plants, we inserted the protein coding sequences of γ-tubulin and cell division controlling E2FA and cell fate determining MYB66 transcription factors into vectors with appropriate tags that enable the purification and detection of *in vitro* translated proteins (Table S3). The obtained pull-down results demonstrated that γ-tubulin and E2FA form a complex even under stringent washing conditions, while no detectable amount of γ-tubulin is associated with the MYB66-coated magnetic beads (Fig. 1A).

Next, we co-translated hexaHis-labelled γ-tubulin and GST-tagged E2FA, E2FB and E2FC proteins for pull-down experiments and showed that all three E2Fs have the ability to interact with γ-tubulin (Fig. 1B). To study whether the presence of E2F dimerization partners disrupts the γ-tubulin/E2F interaction, we added DPA and DPB containing wheat germ translation extract to the co-translated complexes of E2FA, E2FB or E2FC with γ-tubulin and subsequently isolated the E2F protein complexes by glutathione-coated magnetic beads. As shown in Fig. 1B, the amount of γ-tubulin in complex with E2Fs was not reduced after addition of DPs and the DPs simultaneously with γ-tubulin associated with E2Fs. Furthermore, the detection of DP proteins in the unbound fraction of pull-down experiments hints that even a surplus of DPs cannot disrupt the already formed γ-tubulin/E2F complexes (Fig. 1B). Together our data suggest that binding of γ-tubulin and DP to E2Fs is independent and the proteins may form a heterotrimeric complex.

To test whether the dimerization domain (DD) on the E2Fs is required for the γ-tubulin interaction, we prepared constructs to *in vitro* translate C-terminally truncated E2Fs up to the DNA binding domain. Indeed these E2Fs without the dimerization domains; $E2FA^{\Delta DD}$, $E2FB^{\Delta DD}$, and $E2FC^{\Delta DD}$, lost the ability to associate with DPB (Fig. 2A). However, all three truncated E2Fs could still bind to γ-tubulin in pull-down assays, suggesting that plant E2Fs do not require the DD for interaction with γ-tubulin (Fig. 2B). These data further support that γ-tubulin and DP are able to simultaneously associate with E2Fs and form a ternary complex.

γ-Tubulin forms complex with E2FA, E2FB, and E2FC *in vivo*

To study whether plant E2Fs may interact with γ-tubulin *in vivo*, we utilized transgenic Arabidopsis plants expressing GFP-tagged E2FA (pgE2FA-GFP lines 81, 82), E2FB (pgE2FB-GFP line72) and E2FC (pgE2FC-GFP line 2/8/3) under the control of their respective own promoters. Because sucrose can have an effect on E2F activity, we treated seedlings with 2% sucrose or no sucrose for 6 h (Magyar *et al.*, 2012). We then immunopurified E2FA- and E2FB- and E2FC-GFP through the GFP tag and tested for the presence of DPA and DPB proteins and γ-tubulin (Fig. 3A). As expected, the E2F-GFP proteins together with the DPs were enriched in the GFP pull-down compared to the crude extract. In agreement with our *in vitro* data (Figs. 1 and 2), γ-tubulin was also detectable in association with E2FA-, E2FB- and E2FC-GFP, however, as opposed to DPs, it was clearly less abundant in the immunoprecipitate than in the crude extract. This suggests that only a minor portion of the total γ-tubulin pool associates with E2FA, E2FB, and E2FC *in vivo*. The amount of γ-tubulin co-IP with E2Fs did not consistently differ in the presence or absence of sucrose (Fig. 3B), suggesting that the formation of the complex is not affected by conditions that are known to alter RBR phosphorylation and cell proliferation. To rule out that γ-tubulin non-specifically associates with the beads or with the GFP tag, we purified GFP from GFP expressing plants (35S:GFP) and found no detectable γ-tubulin in the GFP pull-down (Fig. 3C). Our data are in agreement with *in vitro* results which show that E2FA, B, and C are able to bind simultaneously the DPs and γ-tubulin (Figs. 1 and 2).

γ-Tubulin is localized together with E2FA in the nuclei

Nuclear localization of plant γ-tubulin was documented by us previously (Binarova *et al.*, 2000; Chumova *et al.*, 2018) and presence of nuclear localization sequence (NLS) and nuclear export sequence (NES) in γ-tubulin supports that its nuclear traffic is regulated (Fig. S1). It was also shown that E2FA is predominantly a nuclear protein (Magyar *et al.*, 2012). We performed TEM immunogold labelling using anti-γ-tubulin antibody in root tips of plants expressing E2FA-GFP under the native promoter. High-pressure freezing and freeze substitution resulted in good preservation of ultrastructure including nuclei (N) (Fig. 4A, B, D). Multiple clusters of γ-tubulin were immunogold labelled on ultrathin sections in the nucleoplasm and sometimes in the nucleolus. Double-immunogold labelling of γ-tubulin and E2FA-GFP showed that some fraction of γ-tubulin and GFP labelling colocalized (Fig. 4C, E, Fig. S2). Two different anti-γ-tubulin antibodies (AthTU and DQ-19) revealed similarly

clustered immunogold labelling pattern that partially colocalized with E2FA-GFP labelling (Fig. 4C, E).

γ-Tubulin binds to promoters of G1/S and G2/M regulators in an E2FA- and E2FB-dependent manner

To investigate whether γ-tubulin is recruited to the promoters of E2F target genes, chromatin immunoprecipitation (ChIP) was performed with Col-0 plants (Fig. 5A). We used conditions when the growth is maximal, 4 h in the light period, or when growth is arrested by a 4 h extended dark period (Graf *et al.*, 2010). We found enrichment of γ-tubulin binding by ChIP on the promoter region of the G1/S regulator *CYCD3;1* and the mitotic *CDKB1;1* in the proliferation promoting light-condition but not in the proliferation repressing dark-condition (Fig. 5A). The enrichment was specific to the region of these promoters where the E2F binding site is located. In the *e2fa-2;e2fb-1* double mutant, the γ-tubulin enrichment with the *CYCD3;1* and *CDKB1;1* promoters was not detectable, suggesting that the E2Fs are required for γ-tubulin recruitment (Fig. 5A). We also tested whether γ-tubulin may associate with the promoter of a typical S-phase specific E2F target, PCNA. For this, we used fully proliferating cultured cells and we found a clear enrichment at the E2F-site of the PCNA promoter compared to no antibody control (Fig. 5B).

The ChIP results are consistent with our protein interaction data on binding of γ-tubulin to the E2F/DP heterodimer *in vitro* and *in vivo*. To investigate whether γ-tubulin alone or as an E2F/DP/γ-tubulin complex may directly bind to DNA with E2F-site, we utilized the Electrophoretic Mobility Shift Assay (EMSA) by applying *in vitro* translated proteins and fluorescently labelled DNA either with the consensus E2F binding site or with E2F-site mutant. As expected, either E2FB or DPB alone could not bind the E2F element, but E2FB/DPB heterodimer did, as shown by the mobility shift with the DNA containing the intact E2F-site. The binding of E2F/DP to DNA was not observed with the mutant E2F element (Fig. S3A). γ-Tubulin alone or together with E2FB did not bind to the E2F-site, suggesting that γ-tubulin/E2F heterodimers have no ability to bind DNA. The addition of γ-tubulin did not alter the binding of E2FB/DPB heterodimer to the E2F-site and the binding was also observed when γ-tubulin was preincubated with E2FB to form a heterodimer and DPB was added later (Fig. S3A). These data indicated an ability of E2F/DP/γ-tubulin heterotrimer to bind to DNA containing E2F-site. Though we were not able to separate the E2F/DP heterodimer and E2F/DP/γ-tubulin heterotrimer by the EMSA, an addition of the

antibody recognizing the His tag fused with γ-tubulin resulted in a supershift of the E2F/DP/γ-tubulin complex (Fig. S3B).

To gain further quantitative evidence on γ-tubulin DNA binding, we also assayed direct protein-DNA association by the Amplified Luminescence Proximity Homogeneous Assay (ALPHA) using biotin labelled DNA and *in vitro* translated proteins. The DNA-E2F interaction was detected by streptavidin donor and Ni chelate acceptor beads and measuring the luminescence signal. In agreement with the results we obtained by EMSA, only the E2FB/DPB heterodimer produced luminescence above the background level with the E2F-site containing DNA, but not with its mutant form. This proximity-generated fluorescence signal between E2FB/DPB heterodimer and the DNA was reduced when γ-tubulin was added (Fig. S4). This observation indicates that γ-tubulin may modulate E2F/DP association with the DNA through ternary complex formation.

Expression of E2F target genes is elevated in plants with reduced γ-tubulin levels

We have found that γ-tubulin forms protein complexes with E2Fs, colocalizes with E2FA in the nucleus, binds to promoters of E2F target genes in an E2F-dependent manner and modulates binding of E2F/DP heterodimer to DNA at the E2F-site. To investigate how the expression of selected E2F target genes is affected by γ-tubulin, we analysed the mRNA levels of genes involved in proliferation and endocycle in seedlings where γ-tubulin was silenced by RNA interference (Binarova *et al.*, 2006). Q-RT-PCR analyses were performed on young newly emerged leaves of WT control and γ-tubulin RNAi plants with mild and strong silencing effects (Fig. 6A). The expression of the *PCNA1*, *ORC2*, *CDKB1;1*, *CCS52A2*, *CYCD3;1* and *RBR* genes were all found to be elevated in comparison to WT and the upregulation of the expression correlated with the strength of γ-tubulin silencing (Fig. 6B). Our data suggest that γ-tubulin acts as a repressor of E2F regulated genes at G1/S and G2/M transitions and at the switch to endocycle.

Silencing of γ-tubulin leads to ectopic cell divisions and enhanced levels of endoreduplication

As we published previously, a reduction of γ-tubulin levels affects cell division in both roots and aerial parts of γ-tubulin RNAi Arabidopsis plants (Binarova *et al.*, 2006). We performed scanning electron microscopy (SEM) and showed that the leaves of γ-tubulin RNAi plants developed rough blade surface as compared to leaves of the WT control that have lobed

pavement cells and regular stomata pattern (Fig. 7A). More detailed inspection of the epidermis of γ-tubulin RNAi leaves by SEM and by immunofluorescence showed that the cellular outcome of γ-tubulin silencing was mixed and both, enlarged isodiametric cells as well as small cells and stomata clusters, were observed (Fig. 7B, C). Contrary to leaf epidermal cells of RNAi plants (Fig. 7B, C) the WT leaves grown in the presence of the anti-microtubular drug, APM, showed only large swollen pavement cells with no lobes, an effect typically found when microtubules are depolymerized (Fig. S5). The consequence of γ-tubulin silencing was also observed in the mesophyll leaf cells. We observed groups of cells with centrally localized large nucleus and dense cytoplasm that were approximately 2.5 times smaller than the average cell size in WT, while there were also cells that were enlarged, appeared vacuolated, a sign that is typical for non-dividing cells (Fig. 7D, E). The population of the small meristematic-like cells showed 4.0 % (n = 3,533) of division while hardly any division was observed in mesophyll cells of the WT control (n = 1,274, Fig. 7D, E).

We applied EdU labelling to visualize DNA replication in γ-tubulin RNAi plants (Fig. 8A, B). After 1 h EdU pulse, large EdU positive nuclei were observed in cotyledons of RNAi plants, but not in the WT cotyledons (Fig. 8A). As expected, many nuclei with uniform size were labelled with EdU in the youngest leaf of the WT seedlings (10 days) after 1 h pulse of EdU treatment. However, in leaves where γ-tubulin was silenced, we observed a mixture of large nuclei with EdU signal and EdU positive nuclei typical for WT leaves at this time point (Fig. 8B). This observation suggests that the enlarged cells with large EdU positive nuclei in the γ-tubulin RNAi line represent cells that prematurely entered endocycle. Further support for over-endoreduplication upon γ-tubulin silencing comes from flow cytometry measurements of DNA content. As compared to WT control, the DNA content was elevated in cotyledons as well as in young leaves of RNAi plants (Fig. 8C). The degree of endoreduplication was quantified by endoreduplication index (EI; the number of endoreduplication cycles per cell). There was an almost 2-fold increase of endoreduplication index in leaves with reduced γ-tubulin levels compared to WT and 1.2-fold increase of EI in cotyledons (Fig. 8D). To prove that the higher DNA content in plants with silenced γ-tubulin is due to endoreduplication and not polyploidy, we counted chromocentra in WT and γ-tubulin RNAi plants. Distribution of cells with the given chromocentra number showed a distinct peak corresponding to the diploid number of chromosomes and was similar for WT and γ-tubulin RNAi leaves (Fig. 8E). Thus, the increased ploidy found upon γ-tubulin silencing is not due to endomitosis, but endoreduplication. The increase in the endoreduplication level shown by microscopical and

flow cytometry data is consistent with the elevated expression of the *CCS52A2* gene upon silencing of γ-tubulin (Fig. 6B).

Altogether, our data showed that γ-tubulin silencing results in overproliferation in some cells while enhanced endoreduplication in others, a phenotype that is reminiscent when E2FA together with DPA is overexpressed (De Veylder *et al.*, 2002; Magyar *et al.*, 2012).

Discussion

The presence of γ-tubulin in plant and animal nuclei suggests non-canonical roles in nuclear processes (Binarova *et al.*, 2000; Chumova *et al.*, 2018, and reviewed in Chumova *et al.*, 2019). Here we provide several lines of evidence that the plant γ-tubulin has functions in the regulation of cell cycle genes in association with E2F transcription factors; i.e. (i) γ-tubulin is in the nucleus and co-localizes with E2F transcription factors, (ii) all canonical Arabidopsis E2F transcription factors; E2FA, E2FB, and E2FC form complexes with γ-tubulin both *in vitro* and *in vivo* and the formation of the complex is independent of the association of these E2Fs with DPs, (iii) γ-tubulin is able to associate, as part of the E2F/DP complex, with the DNA at the E2F-site *in vitro* and it is recruited in an E2F-dependent manner to the promoters of E2F target genes involved in the cell cycle regulation *in vivo*, (iv) the expression of cell cycle E2F target genes, including the G1-to-S regulatory PCNA, ORC2 and CYCD3;1 and the G2-to-M phase specific CDKB1;1 is derepressed in plants with silenced level of γ-tubulin, (v) the observed cellular phenotypes, such as the ectopic cell divisions in some cells, while extra endoreduplication in others, are in line with functions described for E2Fs.

In contrast to what was shown in animal cells (Hoog *et al.*, 2011), we provide evidence that in plants γ-tubulin can interact not only with the activator-type E2Fs, E2FA and E2FB, but also with the repressor type E2FC. Moreover, we find that the dimerization domain is not required for these interactions and in agreement γ-tubulin does not compete with DPs to form an alternative E2F/γ-tubulin heterodimeric complex, but it associates with the E2F/DP dimer to form an E2F/DP/γ-tubulin heterotrimeric complex. This ternary interaction of γ-tubulin with E2F/DP heterodimer might influence the DNA-binding activities of the E2F-DP complexes and/or the formation of repressor complexes. This is consistent with our ChIP data showing that the γ-tubulin association with chromatin is E2F dependent (Fig. 5) and also with our data on the repressive function of γ-tubulin in the regulation of E2F target gene expression (Fig. 6).

In mammalian cells, γ-tubulin was shown to interact with E2F1-3 to repress their activities in order to regulate the G1/S transition following centrosome duplication. Specifically, the repression of CycE expression by γ-tubulin was suggested to have a role in preventing the re-duplication of centrosomes (Hoog *et al.*, 2011). In higher plant cells there are no centrosomes, but the dispersed microtubule nucleation sites containing the γ-tubulin complex are also known to be coordinated via the core cell cycle regulators (Binarova *et al.*, 1998; Weingartner *et al.*, 2001). Here we show that besides the role in microtubule nucleation, γ-tubulin also has a function to form repressor complexes together with the canonical E2F transcription factors and thereby regulate the G1/S control point. Thus this function of γ-tubulin appears to be evolutionarily conserved between animals and plants. However, our findings that γ-tubulin together with E2Fs also regulates the G2/M transition and the endocycle is novel and might be plant specific. Accordingly, while γ-tubulin was only detected in G1 and S phase nuclei of mammalian cells (Hoog *et al.*, 2011), the plant γ-tubulin was detected in nuclei during G1, S as well as the G2 phases of the cell cycle (Binarova *et al.*, 2000). Hence the plant γ-tubulin might have a broader role throughout the cell cycle progression to coordinate microtubule nucleation with cell cycle progression than what was suggested for animal cells. Maintaining the cell division competence is connected with the inhibition of differentiation and the entry into a modified cell cycle with repeated S-phases, called endocycle (Polyn *et al.*, 2015). It was shown that a repressor complex formed around E2FA has an important role in this process (Magyar *et al.*, 2012). Here we present evidence that γ-tubulin, perhaps specifically in plant cells, is also involved in preventing the onset of endocycle.

Plants in which γ-tubulin is silenced show ectopic divisions in some cells while enhanced endoreduplication levels in others in the shoot, a phenotype that was reported for lines when E2FA and DPA were ectopically overexpressed together (De Veylder *et al.*, 2002; Magyar *et al.*, 2012). These two distinct outcomes of γ-tubulin silencing were proposed to depend on the presence or absence of a mitosis inducing factor in different cell types (De Veylder *et al.*, 2002). It was shown that CDKB1;1 is a key E2F target that determines the switch from proliferation to endocycle, and its promoter is controlled by the balance of activator vs repressor type E2Fs (Boudolf *et al.*, 2004). In this work we found that γ-tubulin binds in an E2F-dependent manner to *CDKB1;1* promoter and inhibits its expression. Elevated CDKB1;1 level corroborated with the derepression of other E2F targets, such as *CycD3;1*, should lead to cell divisions, however we find that in some cells there is an extra level of endocycle and cell enlargement. We show that γ-tubulin also represses other E2F target, the *CCS52A* gene, that is involved in endocycle onset which could explain the different outcomes, while there are

DNA replication genes under γ-tubulin control; *ORC2* and *PCNA1* that participate both in normal cell cycle and endocycle.

CCS52A belongs to the Cdh1 protein family, an activator subunit of the anaphase promoting complex (APC) involved in the destruction of mitotic cyclins that is required for the switch from mitosis to endoreduplication (Larson-Rabin *et al.*, 2009; Vanstraelen *et al.*, 2009). E2FA-RBR complex was shown to repress the expression of CCS52As in mitotically active cells to inhibit the entry into endoreduplication (Magyar *et al.*, 2012), and thus the association of γ-tubulin with E2FA to form a repressor complex could explain the extra level of endocycle when γ-tubulin is silenced. Interestingly, γ-tubulin is implicated in the regulation of APC complex in *Aspergillus*, likely acting through Cdh1. The failure of APC inactivation in γ-tubulin mutants prevents mitosis (Edgerton-Morgan and Oakley, 2012, Edgerton *et al.*, 2015).

Emerging other data also underline how cytoskeleton structures can regulate nuclear functions in multiple ways, specifically the chromatin domain organization, DNA repair, and gene expression (Schrank and Gautier, 2019). γ-Tubulin belongs to the tubulin family of proteins and it was demonstrated to have the ability to form oligomers and polymers both in plant and animal cells (Chumova *et al.*, 2018; Lindstrom and Alvarado-Kristensson, 2018). Nuclear and perinuclear γ-tubulin was suggested to have scaffolding and sequestration roles for the nuclear envelope and chromatin organization and in regulation of repair and transcription (rev in Chumova *et al.*, 2019).

In summary, our findings suggest that the coordination of cell cycle gene expression with the spatial and temporal functions of γ-tubulin in microtubular cytoskeleton organization in mitotic and differentiated cells may have an important role in plant development.

Supplementary data

Table S1. List of primers.

Table S2. List of primers used for the construction of truncated E2F proteins.

Table S3. List of *in vitro* translated proteins.

Fig. S1. Protein sequence of Arabidopsis γ-tubulin (At3g61650) with marked nuclear localization signal NLS and NES.

Fig. S2. Ultrastructural immunolocalization of γ-tubulin and GFP-EF2 in nuclei of *A.thaliana* root meristem cells.

Fig. S3. Analysis of the DNA binding capacity of E2F, DP and γ-tubulin by Electrophoretic Mobility Shift Assay.

Fig. S4. Analysis of the DNA binding capacity of different combinations of E2F, DP, and γ-tubulin by ALPHA.

Fig. S5. The effect of antimicrotubular drug APM to leaf pavement cells of Col-0 Arabidopsis plant.

Authors contributions

BK, HK, and JC planned and performed experiments, analysed and interpreted the data and contributed to the manuscript preparation, BK and HK, contributed equally. CP, LT, OK, PH, ZM, and VF performed experiments and analysed the data. PB, LB, ZM, and TM discussed, planned and designed the experiments and discussed the data, PB wrote the manuscript that was completed and finalized together with LB, ZM, and TM.

Acknowledgements

This work was supported by grant P501 15-11657S from Grant Agency of the Czech Republic to P. Binarová and by the Institutional Research Concept RVO 61388971. The research was partially supported by Programme for research and mobility support of young researchers MSM200201901 from Czech Acad. Sci. to H. Kourová, by the Biological and Biotechnology Research Council to L. Bögre (BB/M025047/1), by EFOP-3.6.3-VEKOP-16-2017-00009 to B.M. Kállai, and OTKA-NN-111085 to T. Mészáros, by the grant GINOP-2.3.2-15-2016-00001 from the Ministry of National Economy (Hungary) to Z. Magyar, and by the Czech-BioImaging large RI project LM2015062 MEYS CR and OP RDE CZ.02.1.01/0.0/0.0/16_013/0001775. We thank Barbora Gallová and Anna Kuchařová for help with cloning and selection of γ-tubulin RNAi plants, Gabriela Kočárová for technical assistance, and the CSIRO Plant Industry, Australia for vector pHANNIBAL (Wesley *et al.*, 2001).

References

Binarova P, Cenklova V, Hause B, Kubatova E, Lysak M, Dolezel J, Bogre L, Draber P. 2000. Nuclear gamma-tubulin during acentriolar plant mitosis. The Plant Cell **12**, 433-442.

Binarova P, Cenklova V, Prochazkova J, Doskocilova A, Volc J, Vrlik M, Bogre L. 2006. Gamma-tubulin is essential for acentrosomal microtubule nucleation and coordination of late mitotic events in Arabidopsis. The Plant Cell **18**, 1199-1212.

Binarova P, Hause B, Dolezel J, Draber P. 1998. Association of gamma-tubulin with kinetochore/centromeric region of plant chromosomes. The Plant Journal **14**, 751-757.

Boudolf V, Vlieghe K, Beemster GTS, Magyar Z, Acosta JAT, Maes S, Van Der Schueren E, Inze D, De Veylder L. 2004. The plant-specific cyclin-dependent kinase CDKB1;1 and transcription factor E2Fa-DPa control the balance of mitotically dividing and endoreduplicating cells in Arabidopsis. The Plant Cell **16**, 2683-2692.

Chumova J, Kourova H, Trogelova L, Halada P, Binarova P. 2019. Microtubular and Nuclear Functions of gamma-Tubulin: Are They LINCed? Cells **8**, 259.

Chumova J, Trogelova L, Kourova H, *et al*. 2018. gamma-Tubulin has a conserved intrinsic property of self-polymerization into double stranded filaments and fibrillar networks. Biochimica et Biophysica Acta-Molecular Cell Research **1865**, 734-748.

De Veylder L, Beeckman T, Beemster GTS, *et al*. 2002. Control of proliferation, endoreduplication and differentiation by the Arabidopsis E2Fa-DPa transcription factor. The EMBO Journal **21**, 1360-1368.

Doskocilova A, Kohoutova L, Volc J, *et al*. 2013. NITRILASE1 regulates the exit from proliferation, genome stability and plant development. New Phytologist **198**, 685-698.

Drykova D, Cenklova V, Sulimenko V, Volc J, Draber P, Binarova P. 2003. Plant gamma-tubulin interacts with alphabeta-tubulin dimers and forms membrane-associated complexes. The Plant Cell **15**, 465-480.

Edgerton-Morgan H, Oakley BR. 2012. gamma-Tubulin plays a key role in inactivating APC/C(Cdh1) at the G(1)-S boundary. Journal of Cell Biology **198**, 785-791.

Edgerton H, Paolillo V, Oakley BR. 2015. Spatial regulation of the spindle assembly checkpoint and anaphase-promoting complex in *Aspergillus nidulans*. Molecular Microbiology **95**, 442-457.

Galinha C, Hofhuis H, Luijten M, Willemsen V, Blilou I, Heidstra R, Scheres B. 2007. PLETHORA proteins as dose-dependent master regulators of Arabidopsis root development. Nature **449**, 1053-1057.

Gomez V, Hergovich A. 2014. OLA1 in centrosome biology alongside the BRCA1/BARD1 complex: looking beyond centrosomes. Molecular Cell **53**, 3-5.

Graf A, Schlereth A, Stitt M, Smith AM. 2010. Circadian control of carbohydrate availability for growth in Arabidopsis plants at night. Proceedings of the National Academy of Sciences, USA **107**, 9458-9463.

Hendrickson TW, Yao J, Bhadury S, Corbett AH, Joshi HC. 2001. Conditional Mutations in gamma-Tubulin Reveal Its Involvement in Chromosome Segregation and Cytokinesis. Molecular Biology of the Cell **12**, 2469-2481.

Henriques R, Magyar Z, Monardes A, Khan S, Zalejski C, Orellana J, Szabados L, de la Torre C, Koncz C, Bogre L. 2010. Arabidopsis S6 kinase mutants display chromosome instability and altered RBR1-E2F pathway activity. The EMBO Journal **29**, 2979-2993.
Heyman J, Van den Daele H, De Wit K, Boudolf V, Berckmans B, Verkest A, Alvim Kamei CL, De Jaeger G, Koncz C, De Veylder L. 2011. Arabidopsis ULTRAVIOLET-B-INSENSITIVE4 maintains cell division activity by temporal inhibition of the anaphase-promoting complex/cyclosome. The Plant Cell **23**, 4394-4410.
Hoog G, Zarrizi R, von Stedingk K, Jonsson K, Alvarado-Kristensson M. 2011. Nuclear localization of gamma-tubulin affects E2F transcriptional activity and S-phase progression. FASEB Journal **25**, 3815-3827.
Horejsi B, Vinopal S, Sladkova V, *et al*. 2012. Nuclear gamma-tubulin associates with nucleoli and interacts with tumor suppressor protein C53. Journal of Cellular Physiology **227**, 367-382.
Horvath BM, Kourova H, Nagy S, *et al*. 2017. Arabidopsis RETINOBLASTOMA RELATED directly regulates DNA damage responses through functions beyond cell cycle control. The EMBO Journal **36**, 1261-1278.
Hsieh YW, Alqadah A, Chuang CF. 2016. An Optimized Protocol for Electrophoretic Mobility Shift Assay Using Infrared Fluorescent Dye-labeled Oligonucleotides. J. Vis. Exp. **117**, e54863.
Khan F, He M, Taussig MJ. 2006. Double-hexahistidine tag with high-affinity binding for protein immobilization, purification, and detection on ni-nitrilotriacetic acid surfaces. Analytical Chemistry **78**, 3072-3079.
Kohoutova L, Kourova H, Nagy SK, Volc J, Halada P, Meszaros T, Meskiene I, Bogre L, Binarova P. 2015. The Arabidopsis mitogen-activated protein kinase 6 is associated with gamma-tubulin on microtubules, phosphorylates EB1c and maintains spindle orientation under nitrosative stress. New Phytologist **207**, 1061-1074.
Larson-Rabin Z, Li Z, Masson PH, Day CD. 2009. FZR2/CCS52A1 expression is a determinant of endoreduplication and cell expansion in Arabidopsis. Plant Physiology **149**, 874-884.
Lesca C, Germanier M, Raynaud-Messina B, Pichereaux C, Etievant C, Emond S, Burlet-Schiltz O, Monsarrat B, Wright M, Defais M. 2005. DNA damage induce gamma-tubulin-RAD51 nuclear complexes in mammalian cells. Oncogene **24**, 5165-5172.
Lindstrom L, Alvarado-Kristensson M. 2018. Characterization of gamma-tubulin filaments in mammalian cells. Biochimica et Biophysica Acta-Molecular Cell Research **1865**, 158-171.
Magyar Z, Atanassova A, De Veylder L, Rombauts S, Inze D. 2000. Characterization of two distinct DP-related genes from Arabidopsis thaliana. FEBS Letters **486**, 79-87.
Magyar Z, Bogre L, Ito M. 2016. DREAMs make plant cells to cycle or to become quiescent. Current Opinion in Plant Biology **34,** 100-106.
Magyar Z, De Veylder L, Atanassova A, Bako L, Inze D, Bogre L. 2005. The role of the Arabidopsis E2FB transcription factor in regulating auxin-dependent cell division. The Plant Cell **17**, 2527-2541.
Magyar Z, Horvath B, Khan S, Mohammed B, Henriques R, De Veylder L, Bako L, Scheres B, Bogre L. 2012. Arabidopsis E2FA stimulates proliferation and endocycle separately through RBR-bound and RBR-free complexes. The EMBO Journal **31**, 1480-1493.

Magyar Z, Meszaros T, Miskolczi P, *et al*. 1997. Cell cycle phase specificity of putative cyclin-dependent kinase variants in synchronized alfalfa cells. The Plant Cell **9**, 223-235.
Nagy SK, Meszaros T. 2014. In vitro translation-based protein kinase substrate identification. In: Alexandrov K, Johnston W, eds. Cell-Free Protein Synthesis. Methods in Molecular Biology (Methods and Protocols) Totowa: Humana Press, **1118**, 231-243.
Oakley BR, Paolillo V, Zheng Y. 2015. gamma-Tubulin complexes in microtubule nucleation and beyond. Molecular Biology of the Cell **26**, 2957-2962.
Pastuglia M, Azimzadeh J, Goussot M, Camilleri C, Belcram K, Evrard JL, Schmit AC, Guerche P, Bouchez D. 2006. Gamma-tubulin is essential for microtubule organization and development in Arabidopsis. The Plant Cell **18**, 1412-1425.
Polyn S, Willems A, De Veylder L. 2015. Cell cycle entry, maintenance, and exit during plant development. Current Opinion in Plant Biology **23**, 1-7.
Prigozhina NL, Oakley CE, Lewis AM, Nayak T, Osmani SA, Oakley BR. 2004. Gamma-tubulin plays an essential role in the coordination of mitotic events. Molecular Biology of the Cell **15**, 1374-1386.
Radziejwoski A, Vlieghe K, Lammens T, *et al*. 2011. Atypical E2F activity coordinates PHR1 photolyase gene transcription with endoreduplication onset. The EMBO Journal **30**, 355-363.
Rossello CA, Lindstrom L, Glindre J, Eklund G, Alvarado-Kristensson M. 2016. Gamma-tubulin coordinates nuclear envelope assembly around chromatin. Heliyon **2**, e00166.
Saleh A, Alvarez-Venegas R, Avramova Z. 2008. An efficient chromatin immunoprecipitation (ChIP) protocol for studying histone modifications in Arabidopsis plants. Nature Protocols **3**, 1018-1025.
Schrank B, Gautier J. 2019. Assembling nuclear domains: Lessons from DNA repair. Journal of Cell Biology **218**, 2444-2455.
Umbrasaite J, Schweighofer A, Kazanaviciute V, *et al*. 2010. MAPK phosphatase AP2C3 induces ectopic proliferation of epidermal cells leading to stomata development in Arabidopsis. PLoS ONE **5**, e15357.
Vanstraelen M, Baloban M, Da Ines O, Cultrone A, Lammens T, Boudolf V, Brown SC, De Veylder L, Mergaert P, Kondorosi E. 2009. APC/C-CCS52A complexes control meristem maintenance in the Arabidopsis root. Proceedings of the National Academy of Sciences, USA **106**, 11806-11811.
Vazquez M, Cooper MT, Zurita ME, Kennison JA. 2008. gammaTub23C interacts genetically with Brahma chromatin-remodeling complexes in Drosophila melanogaster. Genetics **108**, 835-843.
Weingartner M, Binarova P, Drykova D, Schweighofer A, David JP, Heberle-Bors E, Doonan J, Bogre L. 2001. Dynamic recruitment of Cdc2 to specific microtubule structures during mitosis. The Plant Cell **13**, 1929-1943.
Wesley SV, Helliwell CA, Smith NA, *et al*. 2001. Construct design for efficient, effective and high-throughput gene silencing in plants. Plant Journal **27**, 581-590.

Figure legends

Fig. 1 γ-Tubulin interacts specifically with E2FA, E2FB, and E2FC *in vitro* and their interaction is not affected by DPs.

(A) *In vitro* translated His_{12}-γ-tubulin was incubated with GST-tagged E2FA and MYB66 transcription factor, glutathione-coated magnetic beads were added to the mixture and the non-specifically bound proteins were removed by washing with either 150 mM or 500 mM NaCl.

(B) The GST-tagged E2FA, E2FB, and E2FC proteins were co-translated with His_6-γ-tubulin and the complexes were isolated by glutathione-coated magnetic beads. The pulled down complexes were complemented with either His_6-DPA or His_6-DPB containing translation mixtures (marked above the blots) to study if the dimerization partner disrupts the E2F-γ-tubulin interaction.

(A, B) Input, bead-bound and unbound proteins were transferred to PVDF membrane and probed with anti-polyHis-POD (upper parts) and anti-GST (lower parts).

Fig. 2 E2F dimerization domain is not essential for γ-tubulin binding.

(A) *In vitro* translated wild type and truncated (ΔDD) GST-tagged E2FA, E2FB, and E2FC proteins were incubated with His_6-DPB and the complexes were isolated by glutathione-coated magnetic beads to demonstrate that His_6-DPB does not bind to the truncated variants of E2Fs.

(B) *In vitro* translated GST, wild type and truncated (ΔDD) GST-tagged E2FA, E2FB, and E2FC proteins were incubated with His_6-γ-tubulin and the complexes were isolated by glutathione-coated magnetic beads to study if the truncated variants of E2Fs can bind His_6-γ-tubulin. Asterisk, non-specific bands.

(A, B) Input and bead-bound proteins were transferred to PVDF membrane and probed with anti-polyHis-POD (upper parts) and anti-GST (lower parts).

Fig. 3 Activator E2FA and E2FB and the repressor E2FC transcription factors interact with γ-tubulin in Arabidopsis seedlings.

(A) Proteins were co-immunoprecipitated (Co-IP) from seedlings (7 das) expressing E2FA-GFP (line 81), E2FB-GFP (line 72) or E2FC-GFP (line 2/8/3) grown with or without sucrose (2% or 0% Suc, respectively) for six hours. Input and co-IP protein samples are indicated on the top left and right side, respectively. W. blot detection with antibodies against GFP, γ-

tubulin, DPA and DPB, indicated on the right side. Arrow, E2FC-GFP. Asterisk, non-specific band. Molecular weight standards are indicated on the left side. Loading control: Coomassie stained proteins on the membrane.

(B) Proteins were co-immunoprecipitated (Co-IP) from seedlings (10 das) expressing E2FA-GFP (line 82) and E2FB-GFP (line 72) grown with or without sucrose (2% or 0% Suc, respectively) for six hours. Input and co-IP protein samples are indicated on the top. W.blot detection with antibodies against GFP and γ-tubulin.

(C) GFP expressing seedlings were used as control. W. blot detection with anti-γ-tubulin antibody (right). GFP is demonstrated by Ponceau staining (left). M, Molecular weight standards.

Fig. 4 Ultrastructural immunolocalization of γ-tubulin and GFP-E2F in nuclei of A. thaliana root meristem cells.

(A) Electron micrograph of a root tip section at low magnification. Arrows: the cells shown at higher magnification in images B and D. Bar: 20 µm.

(B, D) Part of the root cell nucleus double-immunogold labelled with anti-GFP antibody and anti-γ-tubulin antibody DQ-19 (B) or AthTU (D) showing morphology of the cellular compartments. N – nucleoplasm, NL – nucleolus, C – cytoplasm, NE - nuclear envelope. Bar: 500 nm.

(C, E) High magnification of the area shown by rectangle in B or D, respectively. Small gold particles (6 nm, indicated by arrowheads) – E2F-GFP, large gold particles (12 nm) – γ-tubulin (C: DQ-19; E: AthTU). Bar: 100 nm.

Fig. 5 γ-Tubulin binds to promoters of E2F-regulated genes.

(A) ChIP analysis showed γ-tubulin association with promoter regions CDKB1;1 and CycD3 in wild type (WT) plants grown in proliferative conditions (light) but not in the *e2fa-2;e2fb-1* double mutant plants. AthTU antibody was used for IP and DNA regions containing binding sites for E2F (E2F-site) were analysed. Upstream regions were used as negative controls.

(B) ChIP analysis showed γ-tubulin association with promoter regions of E2F-regulated replication gene PCNA in dividing cultured cells Col-0 while there was no binding to CENH3 promotor. No antibody (NoAb) was used as controls.

Error bars indicate standard deviation. A nonparametric Mann-Whitney U test was performed to test for differences between site-specific DNA content in ChIP samples (E2F-site vs. upstream region; **, $P < 0.01$).

Fig. 6 Expression of E2F target genes is upregulated proportionally to the strength of the γ-tubulin RNAi silencing.

(A) Protein level of γ-tubulin in WT and γ-tubulin RNAi (γRNAi) plants (10 das). with mild and strong silencing effects. Proteins in total extract were probed on W. blot with anti-γ-tubulin antibody.

(B) Expression levels of indicated genes were determined by Q-RT-PCR from seedlings of WT and γ-tubulin RNAi plants with mild and strong silencing effects (10 das). A nonparametric Mann-Whitney U test was performed to test for differences between wild type and γ-tubulin RNAi (*, $P < 0.05$; **, $P < 0.01$). Error bars indicate standard deviation of values obtained from three independent experiments in triplicates.

Fig. 7 Silencing of γ-tubulin leads to ectopic division and stomata clustering.

(A) Representative SEM images of leaves of control WT and γ-tubulin RNAi (γRNAi) Arabidopsis plants (12 das).

(B) SEM images, abaxial epidermis of the WT and γ-tubulin RNAi (11 das) with clusters of meristemoids and stomata (arrows) and enlarged isodiametric cells (arrowhead). Bars: 100 µm.

(C) Immunofluorescence labelling of α-tubulin (green) in abaxial epidermis of γ-tubulin RNAi (11 das) with cluster of stomata (arrows) and enlarged isodiametric cells (arrowhead). DNA stained by DAPI (blue). Bar: 100 µm.

(D) Immunofluorescence labelling of α-tubulin (green) in mesophyll cells in WT and γ-tubulin RNAi leaves (11 das) with small proliferating cells (SC, mitosis and cytokinesis marked by asterisks) and enlarged isodiametric cells (EC); DNA stained by DAPI (blue). Bars: 150 µm.

(E) Box plot of cell number counted in randomly selected defined area (1,000 µm x 1,000 µm) of mesophyll cells of WT and γ-tubulin RNAi leaves. Cell numbers are visualized in quartiles of ranked data expressed by means with SD ($n = 22$). Asterisks indicate $P < 0.01$ comparing WT and γ-tubulin RNAi in Student's t-test. Compared to WT with cells of uniform size, two distinct cell populations of small and enlarged cells were demonstrated in γ-tubulin RNAi leaves.

Fig. 8 Elevated level of endoreduplication in plants with silenced γ-tubulin.

(A) Representative images of EdU (1 h pulse) labelling in large nuclei (arrows) in cotyledons of γ-tubulin RNAi (γRNAi) plants (7 das). but not WT control plants EdU (green), DAPI (blue). Bars: 100 µm.

(B) EdU labelling (1 h pulse) in the youngest leaves of the WT and γ-tubulin RNAi plants (10 das). Large EdU positive nuclei (arrows). Bars: 100 µm.

(C) Representative DNA content histograms determined by flow cytometry of WT and γ-tubulin RNAi leaves (13 and 17 das) and cotyledons (13 das).

(D) Endoreduplication index determined from flow cytometry data measured in leaves and cotyledons of WT and γ-tubulin RNAi. Data are represented as mean with SD (n = 8). Asterisk indicates $P < 0.05$ comparing WT and γ-tubulin RNAi in Student's t-test.

(E) Distribution of nuclei with given number of chromocentra in γ-tubulin RNAi (n = 513) and WT leaves (n = 1,091).

Figure 1

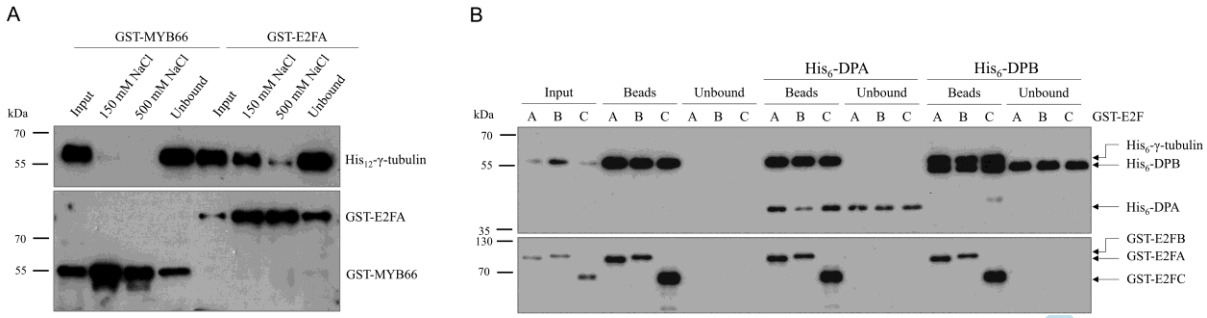

Figure 2

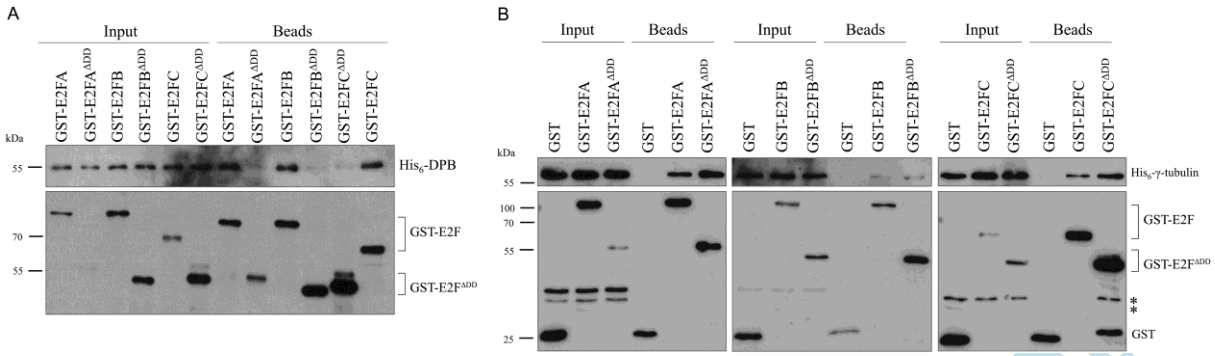

Figure 3

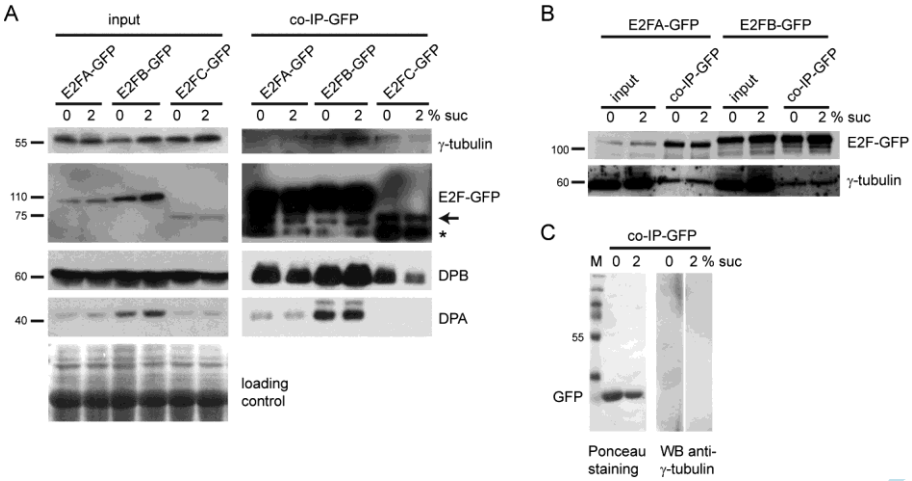

Figure 4

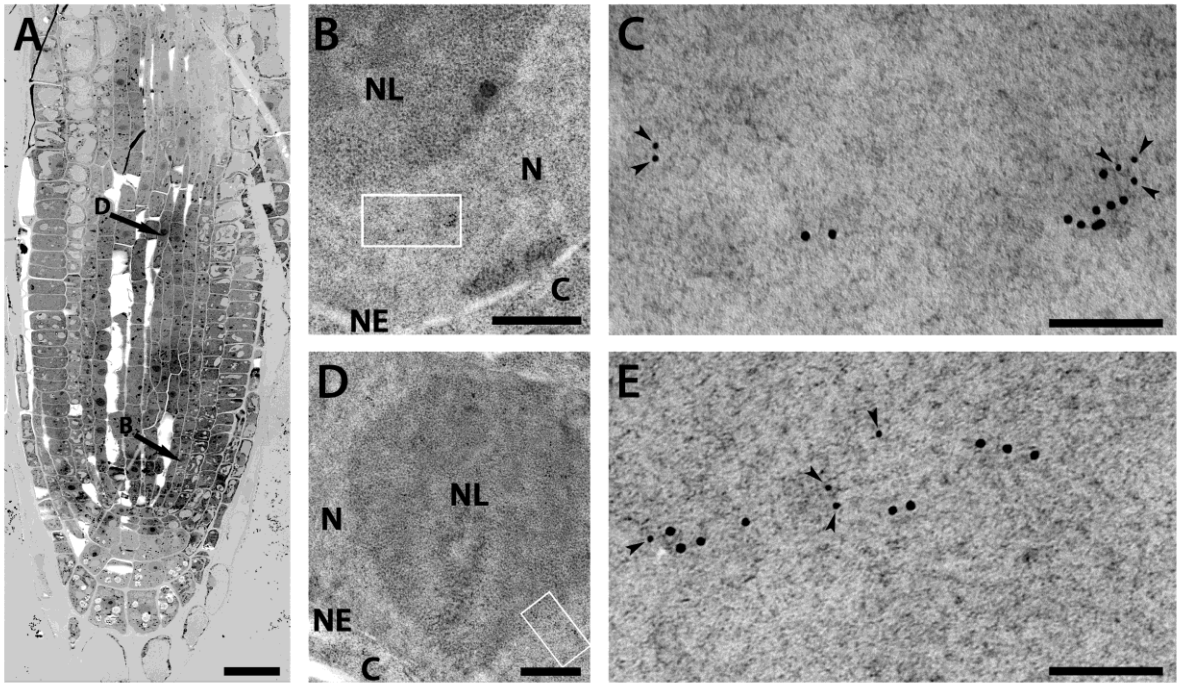

Figure 5

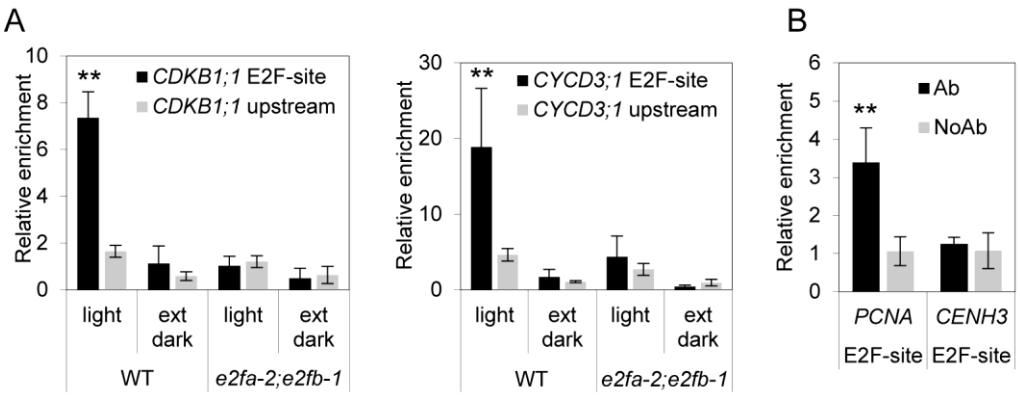

Figure 6

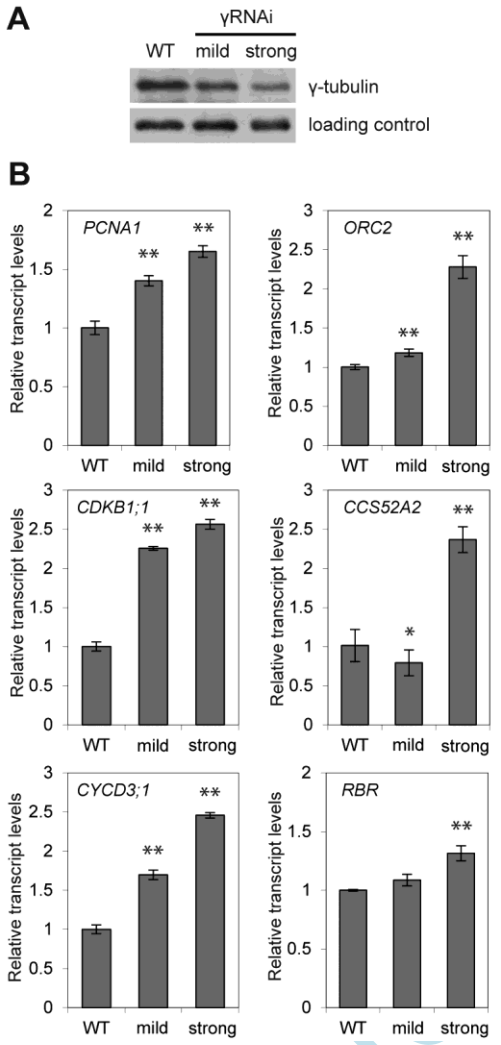

Figure 7

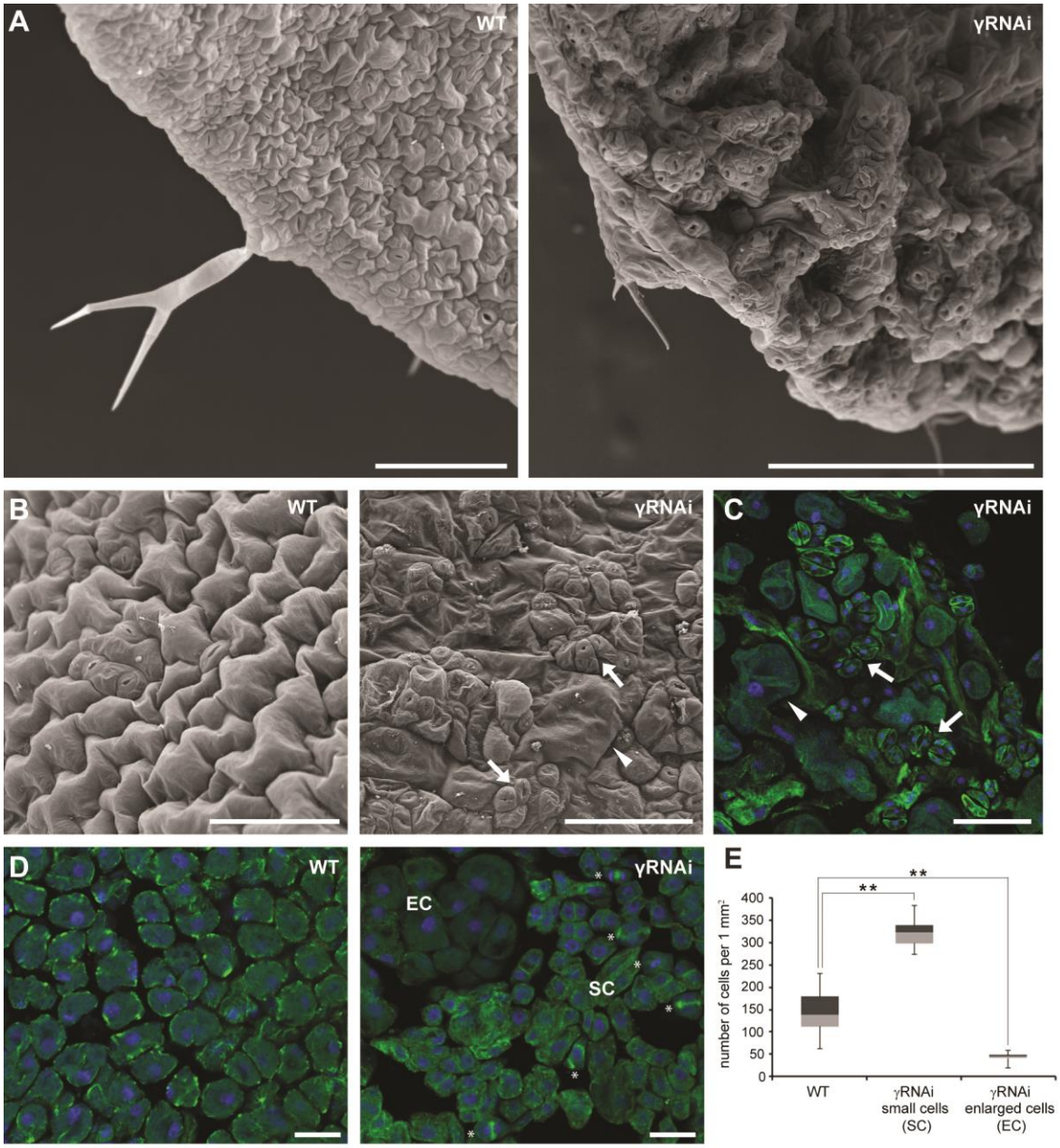

Figure 8